Investigation of AC Resistance on Winding Conductors in Slot According to Strands Configuration

Jun-Woo Chin, Kyoung-Soo Cha, Jin-Cheol Park, Dong-Min Kim, Jung-Pyo Hong, *Senior Member, IEEE*, and Myung-Seop Lim, *Member, IEEE*

***Abstract*—Owing to the high speed and frequency required in electric machine industry, the significance of ac resistance has been increasing. This study investigates the ac resistance of windings according to the configuration of strands. The mechanism of generating the ac resistance in winding conductors was investigated with respect to the slot leakage flux and eddy current. Then, when applying the strands to the winding, the concept of unbalanced impedance was introduced to characterize the additional ac resistance due to circulating current. The analytic method to calculate ac resistance describing the above phenomena is derived and verified by FEA results. Afterward, the ac resistances of varying numbers and arrangements of strands were separately studied via finite element analysis. In addition, a method to avoid increasing the ac resistance was suggested based on impedance equalization when applying strands. Finally, experiments were conducted to verify the effect of the strand configuration on ac resistance. An E- and I- shaped core, which can be the rendering of common electric machines, such as motors, generators, and transformers, was manufactured and tested with winding specimens. Consequently, the test results showed a similar trend as the analytical results.**

***Index Terms*—AC resistance, circulating current, eddy current, impedance, slot leakage flux, slot leakage inductance, strand, transposition.**

I. Introduction

As THE demand for downsizing and high power density is increasing in the electric machine industry, machines need to operate in high speed and high-frequency systems to satisfy these requirements. However, in the case of electric motors using alternating current (ac), a size reduction decreases the output torque because size is proportional to output torque. Hence, to generate the same output power, the speed should be increased instead of the reduction of the output torque. This leads to an increase of the system's frequency, which causes the system's voltage to rise [1], [2].

Moreover, as the frequency of the system increases, the losses in the transformer and rotating electrical machine increase. In high-frequency operations, the increase in the iron loss, which occurs at the iron core, is proportional to the square of the frequency. Consequently, only the iron loss is thought to be important; however, the copper loss also increases with higher frequency because of the skin and proximity effects in the winding, which contribute to the ac resistance.

With respect to the thermal characteristics, an increase in the copper loss can cause much more serious problems than the iron loss. In the stator core, where the temperature rises due to iron loss, heat dissipates well through the housing. However, in the winding, where the temperature increases due to copper loss, heat dissipation is difficult owing to the contact state between the winding and stator core. Consequently, the rise in temperature of the winding increases the resistance of the winding, and it can deteriorate the rotating electrical machine [3]–[6]. Therefore, it is important to estimate the ac resistance of the winding.

Recently, several studies on various applications considering AC resistance have been conducted. The AC losses in tooth-coil winding permanent magnet synchronous motors (PMSMs) have been investigated using the finite element analysis (FEA) method [7]. Additionally, in electric vehicle and hybrid electric vehicle applications, the AC resistance in the stator winding of the PMSM has been studied via FEA [8]. In addition, various PMSM designs, which consider, the AC resistance were proposed for the traction of electric vehicles [9], [10]. Moreover, the analytical methods and design guidelines of hairpin windings for high-performance electric vehicle motors were researched by N. Bianchi and G. Berardi, respectively [11], [12].

Not only for applications, but also for theories, studies about the effects of applying strands and circulating current between strands on ac resistance have done by a few researchers. Jiancheng proposed the analytic method to calculate the circulating current loss generating additional ac resistance for high-speed permanent magnet motor [13]. However, the proposed method assumes arrangement of all the conductors and strands

Manuscript received May 8, 2020; revised September 28, 2020; accepted October 20, 2020. Date of publication October 26, 2020; date of current version December 31, 2020. Paper 2020-EMC-0799.R1, presented at the 2019 IEEE Energy Conversion Congress and Exposition, Baltimore, MD, USA, May 20–24, and approved for publication in the IEEE Transactions on Industry Applications by the Electric Machines Committee of the IEEE Industry Application Society. This work was supported by the National Research Foundation of Korea grant funded by the Korea government (MSIT) (NRF-2020R1A4A4079701). *(Corresponding author: Myung-Seop Lim.)*

The authors are with the Department of Automotive Engineering, Hanyang University, Seoul 04763, South Korea (e-mail: cjw1254@hanyang.ac.kr; chakungsoo@hanyang.ac.kr; skensk1990@hanyang.ac.kr; kimdmin@hanyang.ac.kr; hongjp@hanyang.ac.kr; myungseop@hanyang.ac.kr).

Color versions of one or more of the figures in this article are available online at https://ieeexplore.ieee.org.

Digital Object Identifier 10.1109/TIA.2020.3033815

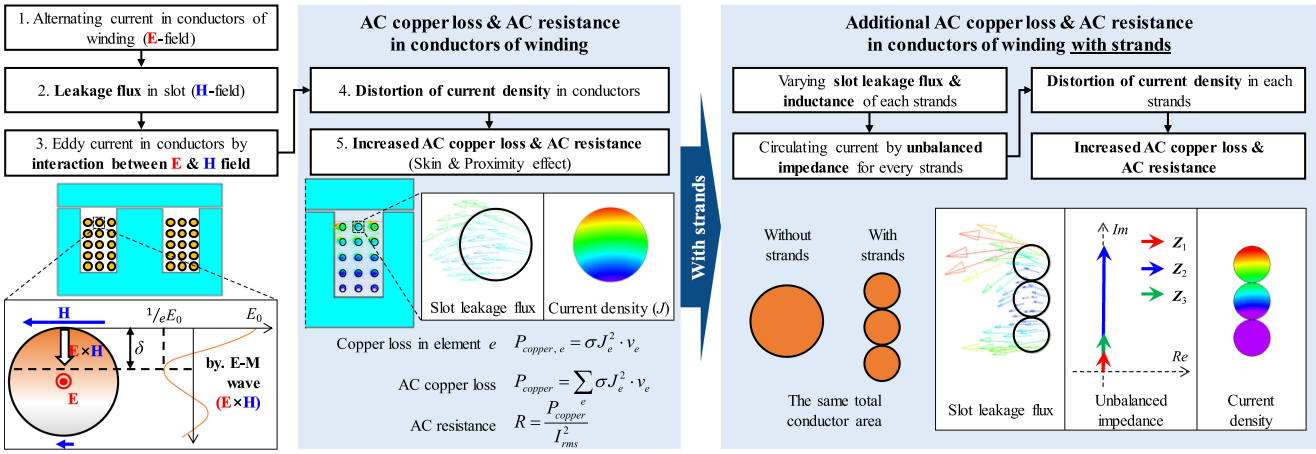

Fig. 1. Mechanism of occurring ac resistance in conductors of winding without and with strands.

as one-dimensional model in succession along the center line, so that it cannot be generalized. Another research, conducted by van der Geest, studied the postprocess to calculate ac resistance based on FEA results [14]. This study contains the effect of strands arrangement on ac resistance, but effectiveness of strands transposition was not investigated theoretically and not verified by experiment.

Studies on ac resistance have been actively conducted. Hanselman and Lipo derived the analytic solution for the ac resistance of a rectangular wire connected in series that fits fully within the width of the slot, respectively [15], [16]. Additionally, Pyrhonen suggested an analytic solution for the ac resistance of a rectangular wire connected in series that does not fit fully within the width of the slot [17]. However, studies on ac resistance in cases where round wire and strands are applied to the winding are inadequate.

In this study, the ac resistance of the winding conductors in slot was investigated with respect to the number and arrangement of strands. First, the mechanism of the ac resistance in the winding conductors in the slot was studied from the concept of slot leakage flux. When the strands are applied to the winding conductors, the ac resistance induced by circulating current is added because each strand has a different impedance owing to the slot leakage inductance. Then, the analytic method to calculate ac resistance describing above phenomena is derived and verified by FEA results. In addition, the ac resistances of varying numbers and arrangements of strands were separately analyzed and compared via FEA. Moreover, transposition, the method to avoid increasing the ac resistance by equalizing the impedance of strands, was used when applying strands, and the results were compared with the former ones. Finally, experiments were conducted to verify the effect of the number and arrangement of strands on ac resistance. To investigate a situation similar to that in widely used electric machines, such as motors, generators, and transformers, an E- and I- shaped iron core was manufactured and tested with winding specimens. In winding specimens, a strand arrangement representing actual applications was used and tested. Moreover, the effect of transposition on preventing the rise in ac resistance was verified experimentally too.

II. AC Resistance of Winding Conductors in Slot

If a winding is surrounded by an iron core and an ac current flows, the current causes the slot leakage flux to alternate; consequently, ac resistance is generated. Fig. 1 illustrates how the ac resistance occurs in winding conductors in slots with or without strands.

When an ac current flows along the winding conductors in slots without strands, it produces an electric field in the conductor and a magnetic field surrounding the conductor as per Ampere's law. This magnetic field also exists in the slot as leakage flux and it passes through the conductors in the slot. From the interaction of the electric and magnetic fields in the conductor, an eddy current occurs, which distorts the current density in the conductors. This phenomenon causes not only the copper loss but also the resistance of the conductor to increase; this process can be expressed as the skin and proximity effects of ac resistance [7].

However, when the strands are applied to the winding conductors in the slot, an additional phenomenon increases the ac resistance. Based on the arrangement of strands, the slot leakage flux varies and the slot leakage inductance differs from strand to strand. This variation in the slot leakage inductance unbalances the impedance of each strand, which distorts the current density in each strand. As mentioned above, this type of distortion also causes the ac resistance to increase.

Using the slot leakage flux, the mechanisms of generating ac resistance in winding conductors in slots with or without strands were characterized. Next, the analytic method of ac resistance for winding conductors applying strands is derived in the following section. Then, the ac resistance according to variation in the number and arrangement of strands were separately analyzed via FEA. When investigating the ac resistance in winding conductors in slots, the common analysis conditions are shown in Fig. 2 and Table I. The winding is wound around

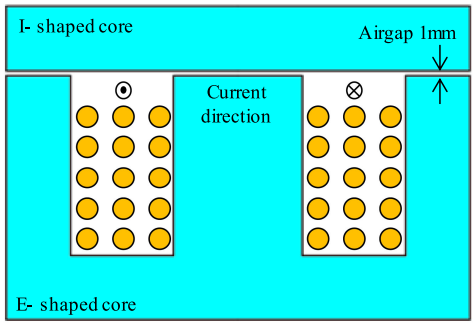

Fig. 2. E- and I- shaped core with winding.

TABLE I
ANALYSIS CONDITION OF WINDING WITH E- AND I-SHAPED CORE

ITEM	UNIT	VALUE
Input current	A_{rms}	24
Frequency	Hz	Varying
Number of winding turns	-	15
Number of strands	-	Varying
Airgap	mm	1
Core material	-	50PN470
Core stack length	mm	50

E- and I- shaped core, and the airgap between E- and I- shaped core is 1 mm.

III. ANALYTIC METHOD OF AC RESISTANCE FOR WINDING CONDUCTORS IN SLOT

Many researchers have studied ac resistance of the coil. In particular, Pyrhönen studied an analytical approach for determining the ac resistance of a series-connected rectangular wire by applying the concept of circuit analysis in section "5.2 Influence of Skin Effect on Resistance" in his book [17]. However, this study only dealt with the rectangular conductors, and their turns and strands arrangement are limited so that the proposed analytical approach cannot be applied to generalized shape and arrangement of conductors, turns, and strands. Therefore, to overcome these limitations, the analytical method to calculate the ac resistance of winding conductors in slot based on the prestudied analytical approach [17] is derived in this section. When examining the ac resistance, two phenomena occur simultaneously: 1) the ac resistance due to the conductors of a row of turns itself and 2) the ac resistance owing to the conductors of the other row of turn. The former can be inferred as skin effect and the latter can be interpreted as the proximity effect and circulating current.

A. AC Resistance Due to the Conductors of a Turn Itself

As shown in Fig. 3, there is a generalized strand arrangement for a row of turns. In this study, the conductors of strands are divided into *n* imaginary layers (or subconductors) as depicted in Fig. 3. Also, there are assumptions as follows:

1) It is assumed that skin effect does not occur inside a subconductor.

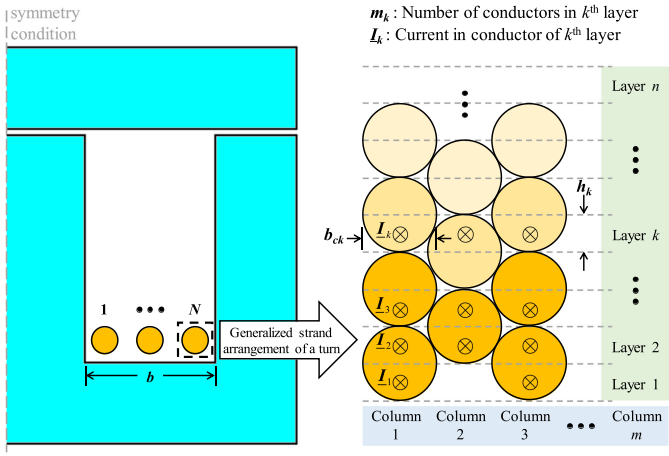

Fig. 3. Analytic model of generalized strand arrangement of a row of turns.

2) The currents are flowing along the center lines of the subconductors.
3) The slot leakage flux only flows in the *x*-direction.

In the steady state, the complex form of voltage induced in the *k*th subconductor by the slot leakage flux is

$$\underline{E}_k = -j\omega\Delta\underline{\Phi}_k = R_k\underline{I}_k - R_{k+1}\underline{I}_{k+1} \tag{1}$$

where $\Delta\underline{\Phi}_k$ is the leakage flux flowing between the *k*th and $(k+1)$th subconductors, $\underline{I}_k$ and $\underline{I}_{k+1}$ are the currents in subconductors k and $k+1$, and ω is the angular velocity. The induced voltage creates a circulating current limited by the resistances R_k and R_{k+1} of the layers.

The flux density B_k in the subconductor k between the currents $\underline{I}_k$ and $\underline{I}_{k+1}$ depends on the current linkage Θ_k calculated from the bottom of the slot to the subconductor k

$$B_k = \mu_0\frac{\Theta_k}{b_k} = \mu_0\frac{1}{b_k}\sum_{\gamma=1}^{k} m_\gamma i_\gamma \tag{2}$$

where b_k is the width of the slot at the position of the *k*th subconductor and m_γ is the number of subconductors in the γth layer. The partial flux through the area limited by the paths of the currents $\underline{I}_k$ and $\underline{I}_{k+1}$ is

$$\Delta\Phi_k = B_k l h_k = \mu_0\frac{\Theta_k}{b_k} l h_k = \mu_0\frac{l h_k}{b_k}\sum_{\gamma=1}^{k} m_\gamma i_\gamma \tag{3}$$

where l is the axial length of the iron core and h_k is the height of the *k*th subconductor.

By substituting (3) into (1), and by employing phasors, we obtain

$$\underline{E}_k = -j\omega\mu_0\frac{N l h_k}{b_k}\sum_{\gamma=1}^{k} m_\gamma i_\gamma = R_k\underline{I}_k - R_{k+1}\underline{I}_{k+1}. \tag{4}$$

Next, the current is solved as follows:

$$\underline{I}_{k+1} = \frac{R_k}{R_{k+1}}\underline{I}_k + \frac{j\omega\mu_0}{R_{k+1}}\frac{N l h_k}{b_k}\sum_{\gamma=1}^{k} m_\gamma i_\gamma. \tag{5}$$

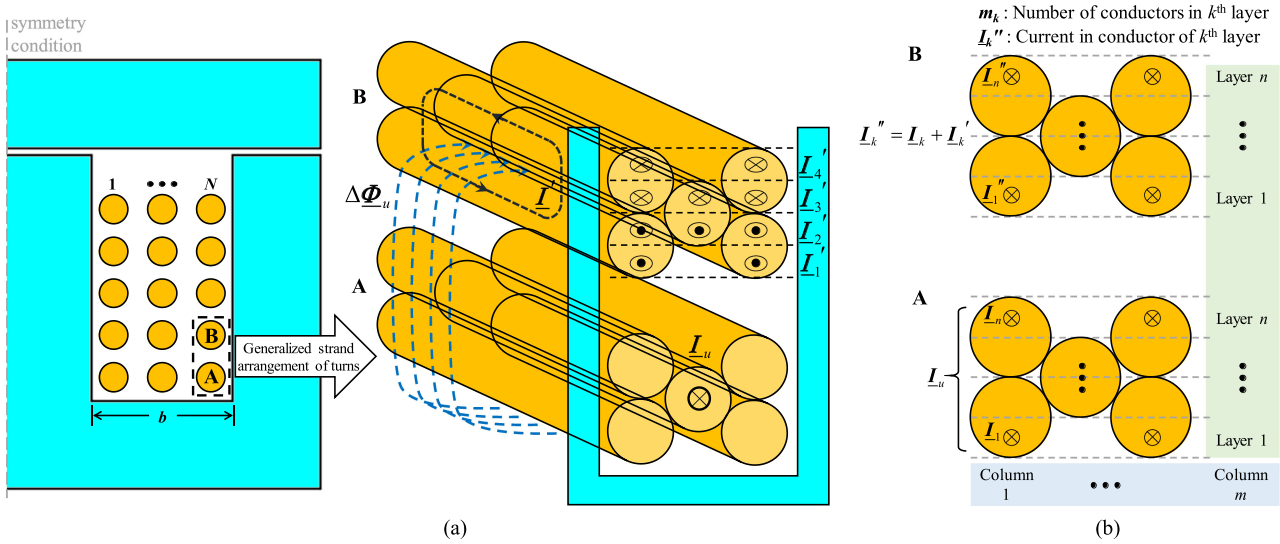

Fig. 4. Analytic model of generalized strand arrangement of several rows of turns in winding. (a) Current caused by the flux of underlying turns. (b) Sum of currents caused by the flux of itself and underlying turns.

Normally, the total current of all the subconductors is given, all the currents of subconductors are determined by (5) and (6)

$$\underline{I}_{\text{total}} = \sum_{k=1}^{n} \underline{I}_k. \tag{6}$$

For now, there was only one row of turns in winding and ac resistance was generated by itself. The following section will handle the effect on ac resistance of upper rows of turns by lower rows of turns in winding.

B. AC Resistance Due to the Conductors of the Other Turn

When there are several rows of turns in winding, not only the ac resistance of the turns itself, but also the ac resistance of the turns by other turns should be taken into account. Fig. 4 shows the analytic model of the generalized strand arrangement of several rows of turns in winding. As shown in Fig. 4, the uppermost turn experiences the composed flux generated by itself and by lower turns. The upper turn that is divided into imaginary layers (or subconductors) experiences a flux created by a lower turn. This makes the investigation of the ac resistance of the upper turn somewhat more complex than in the previous case.

The currents of the subconductors k in the upper turn have to be divided into two imaginary sections: $\underline{I}_k$, which would be the current of the subconductor k if its row of turns were alone in the slot (derived in the previous section); and $\underline{I}_k{}'$, caused by the flux of the underlying rows of turns. That is

$$\underline{I}''_k = \underline{I}_k + \underline{I}'_k. \tag{7}$$

The currents of the lower turn $\underline{I}_u$ create a time-varying magnetic flux density in the area of the upper turn. The eddy current pattern created by this flux density has to be symmetrical with respect to the center line of the upper turn. Consequently, it is advisable to divide the upper turn into an even number of subconductors as shown in Fig. 4(a). The subconductors of the upper turn carry eddy currents that, according to Lenz's law, attempt to cancel the flux created by the lower turn current. Therefore, the eddy current components at equal distances below and above the center of the conductor have to be equal in magnitude and opposite in directions

$$\underline{I}'_k = -\underline{I}'_{n-k+1}. \tag{8}$$

As shown in Fig. 4(a), the currents $\underline{I}_1{}'$ and $\underline{I}_2{}'$ travel toward the observer, and the currents $\underline{I}_3{}'$ and $\underline{I}_4{}'$ run in the same direction as the sum of currents of the lower turn.

The flux created by the current $\underline{I}_u$ of the lower turn induces a current $\underline{I}'_{k+1}$ in the upper subconductor $k+1$. This current can be calculated in the $(k+1)$th imaginary subconductor analogously according to (5)

$$\underline{I}'_{k+1} = \frac{R_k}{R_{k+1}}\underline{I}'_k + \frac{j\omega\mu_0}{R_{k+1}}\frac{Nlh_k}{b_k}\left(\sum_{\gamma=1}^{k} m_\gamma \underline{I}'_\gamma + \underline{I}_u\right). \tag{9}$$

With the even n, the subconductors $k = n/2$ and $k+1 = n/2+1$ constitute the center of the turn. Here, we may write for the currents, according to (9)

$$\begin{aligned}\underline{I}'_{n/2+1} = -\underline{I}'_{n/2} &= \frac{R_{n/2}}{R_{n/2+1}}\underline{I}'_{n/2} \\ &\quad + \frac{j\omega\mu_0}{R_{n/2+1}}\frac{Nlh_{n/2}}{b_{n/2}}\left(\sum_{\gamma=1}^{n/2} m_\gamma \underline{I}'_\gamma + \underline{I}_u\right) \\ &= \frac{R_{n/2}}{R_{n/2+1}}\underline{I}'_{n/2} + \frac{j\omega\mu_0}{R_{n/2+1}}\frac{Nlh_{n/2}}{b_{n/2}}\underline{I}_\mu \\ &\quad \left(where,\ \underline{I}_\mu = \sum_{\gamma=1}^{n/2} m_\gamma \underline{I}'_\gamma + \underline{I}_u\right).\end{aligned} \tag{10}$$

Equation (10) can be summarized for the subconductor $k = n/2$ lying below the center line of the upper turn

$$\underline{I'}_{n/2} = -\frac{j\omega\mu_0}{R_{n/2+1}}\frac{Nlh_{n/2}}{b_{n/2}}\underline{I}_{\mu} = -\frac{j\omega\mu_0}{R_{n/2+1}}\frac{Nlh_{n/2}}{b_{n/2}}\left(\sum_{\gamma=1}^{n/2} m_{\gamma}\underline{I'}_{\gamma} + \underline{I}_{u}\right). \quad (11)$$

We now write for the other lower subconductors of the upper turn, according to (9)

$$\underline{I'}_{n/2-1} = \frac{R_{n/2}}{R_{n/2-1}}\underline{I'}_{n/2} - \frac{j\omega\mu_0}{R_{n/2-1}}\frac{Nlh_{n/2-1}}{b_{n/2-1}}\left(\sum_{\gamma=1}^{n/2-1} m_{\gamma}\underline{I'}_{\gamma} + \underline{I}_{u}\right) = \frac{R_{n/2}}{R_{n/2-1}}\underline{I'}_{n/2} - \frac{j\omega\mu_0}{R_{n/2-1}}\frac{Nlh_{n/2-1}}{b_{n/2-1}}\left(\underline{I}_{\mu} - m_{n/2}\underline{I'}_{n/2}\right). \quad (12)$$

Since the currents of the underlying rows of turns $\underline{I}_u$ is known for every row of turns in winding, the current $\underline{I}_k{}'$ caused by the flux of the underlying rows of turns can be calculated by iteration. Finally, the currents of the subconductors k in the upper turn can be obtained by (7).

With the current $\underline{I}_k{}'$ and resistance R_k, the total copper loss of winding can be calculated and also the ac resistance of the winding can be calculated by dividing the rms input current. Then, the resistance factor (R/R_{DC}), which means the ratio of ac resistance to dc resistance, can be obtained. The results of resistance factor by analytic method will be compared with FEA results in the following section.

IV. AC Resistance According to the Configuration of Strands

To analyze the ac resistance according to the configuration of strands, the number and the arrangement of strands were studied in this section. Moreover, the variation in the ac resistance with respect to the configuration of strands was analyzed using circuit impedance. Furthermore, the arrangement of strands that can decrease the ac resistance was investigated. To perform a proper comparison, the following assumptions were used.

1) DC resistance of coil side is the same regardless of the number of strands.
2) AC resistance of end coil is ignored, and only dc resistance of end coil is considered.

A. Varying the Number of Strands

When studying the ac resistance according to the number of strands, the condition that the total height (2.3 mm), width (2.3 mm), and area (4.15 mm^2) of a turn are the same before and after the strand is applied. To satisfy the above conditions, the number of strands should be a square number. Fig. 5 shows the strand arrangement for no, four, and nine strands. The orders of arrangement for strands are the same along the turns. In addition, the input current is 24A$_{\mathrm{rms}}$ with a sinusoidal waveform. In this section, only the resistance of the coil side is considered.

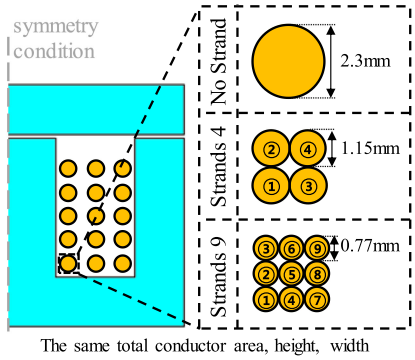

Fig. 5. Strand arrangement according to the number of strands.

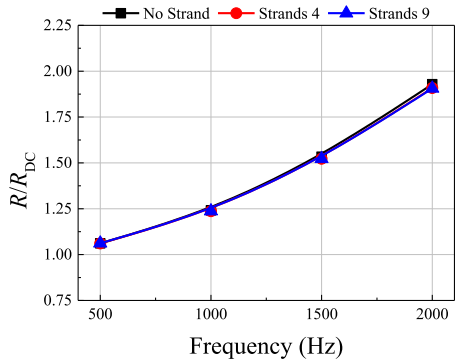

Fig. 6. FEA results of R/R_{DC} according to the number of strands.

Fig. 6 shows the two-dimensional (2-D) FEA results of the ac resistance according to the number of strands. The resistance factor becomes larger at higher frequencies. Additionally, the resistance factors are almost the same according to the number of strands because the total height, width, and area of a turn according to the number of strands are the same.

As shown in Fig. 7, the current density distribution of turns differs along the row direction owing to the eddy current in the conductors. The time derivative of slot leakage flux causes an eddy current in the conductor; this current is larger in the upper turn than in the lower turn according to Ampere's circuit law. Therefore, the current density is larger in the upper turn. In addition, the current density distributions of the conductors are similar according to the number of strands. Hence, almost the same resistance factors are obtained with respect to the number of strands.

B. Varying the Arrangement of Strands

In contrast, it is impossible to achieve the same height and width of a turn according to the number of strands, as shown in the previous section. To investigate the cases that reflect the actual winding situation, the various arrangements of strands 3

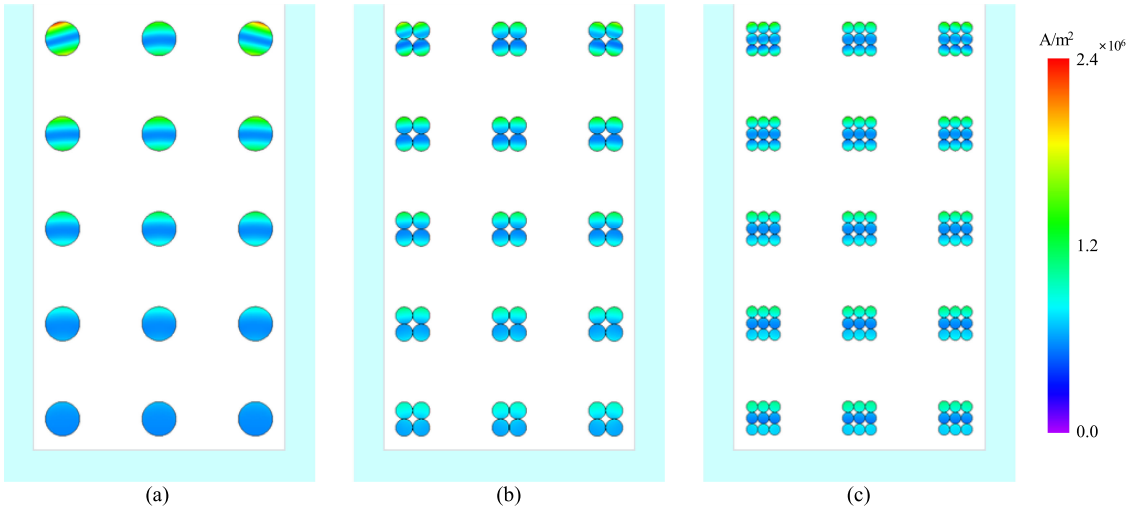

Fig. 7. RMS value of current density for conductors according to the number of strands at 2000 Hz (FEA). (a) No strand. (b) Strands 4. (c) Strands 9.

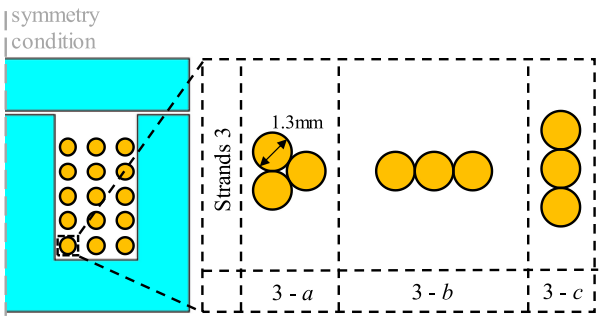

Fig. 8. Varying strands arrangement.

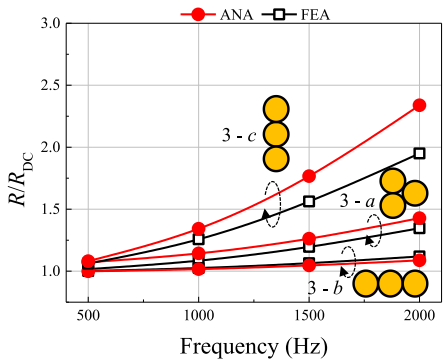

Fig. 9. Analytic and FEA results of R/R_{DC} with varying strands arrangement.

are considered as shown in Fig. 8. Case 3 - *a* is a representative of the actual case with three strands. This case represents the arrangement of strands that is used in reality when winding coil. However, the arrangement of strands in reality can be similar to that in case 3 - *a* and/or 3 - *c* because of the tension generated when winding. Therefore, it is important to investigate the ac resistance for various cases ranging from 3 - *a* to 3 - *c*. The order of arrangement for strands is the same along the turns. In this section, the resistances of the coil side and end coil are considered. Particularly for the end coil, the dc resistance is applied as the measured value and the ac resistance is ignored.

Fig. 9 shows the results of ac resistance by analytic method and 2-D FEA for various arrangement cases. For the case 3 - *b*, the results of the analytic method and FEA are almost similar according to the frequency, but the case 3 - *a* and - *c* are not. It is because the analytic method only considers slot leakage flux in the *x*-direction. On the other hand, the FEA results reflect the influence of slot leakage flux in the *y*-direction as can be seen in Fig. 10. It can be inferred that case 3 - *a* and 3 - *c* have much more *y*-direction of slot leakage fluxes compared to 3 - *b* in the uppermost turns.

Unlike the cases in Section IV-A, the resistance factors differ according to the arrangement of strands. The differences in ac resistance with varying strand arrangements can be explained logically from the viewpoint of impedance. Fig. 11 shows the impedance circuit for strands. If the position in the row direction of the strands is the same as shown in case 3 - *b*, the slot leakage flux and inductance become similar along the strands. This means that the impedance of each strand is similar as shown in Fig. 12(b). However, if the position in the row direction of the strands is different like in case 3 - *a* and 3 - *c*, the slot leakage flux and inductance in the upper strand differ from that in the lower strand. This implies that the impedance of each strand is different as shown in Fig. 12(a) and (c). Consequently, this results in circulating current between strands and causes the copper loss to rise.

C. *Effect of Strand Transposition*

From the results of Section III-*B*, the ac resistance can be a critical problem if the arrangement of strands in reality is similar to that in case 3 - *c*. Thus, it is essential to reduce the resistance factor when applying strands in windings. Therefore, in this study, transposition, which is widely used in large generator applications, transformer applications, and inductors like Roebel

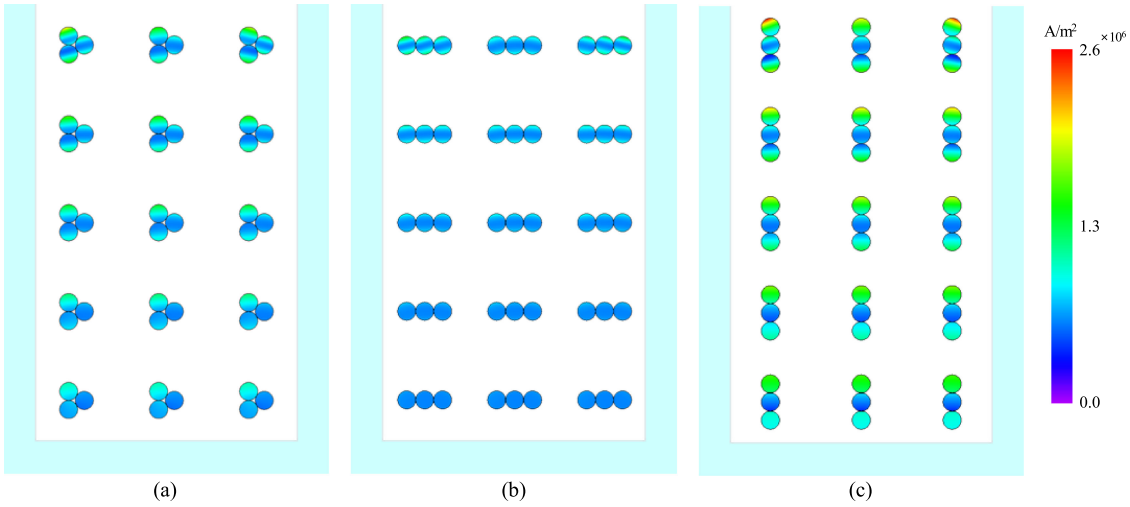

Fig. 10. RMS value of current density for conductors varying strand arrangement at 2000 Hz (FEA). (a) 3 - *a*. (b) 3 - *b*. (c) 3 - *c*.

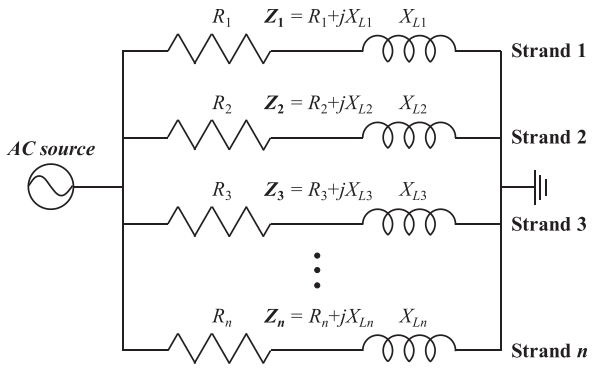

Fig. 11. Impedance circuit for winding with strands.

bar, is suggested to reduce the resistance factor [18]–[21]. Moreover, not only full-transposition, but also partial-transposition can be an effective method to avoid increasing the ac resistance. Fig. 13 shows strand arrangements without and with transposition in the case of three strands (case 3 - *a* and case 3 - trans.). In this section, the resistances of coil side and end coil are both considered. Especially for the end coil, the dc resistance is applied as the measured value and the ac resistance is ignored.

Figs. 14 and 15 show the 2-D FEA results of the ac resistance for the nontransposed and transposed cases. As shown in Fig. 14, the resistance factor of the transposed case (3 - trans.) is much lower compared to the nontransposed case (case 3 - *a*). In addition, the current density distribution can be seen in Fig. 15, which indicates that the transposed case has much lower values of current density than that of the nontransposed case.

Similar to the explanation provided in Section III-B, the decrease in ac resistance due to transposition can be explained from the viewpoint of impedance. Fig. 16 shows the impedance of each strand. As transposition is applied to the winding, the average slot leakage flux and inductance become similar along the strands. As shown in Fig. 16(b), this results in the equivalence of the impedances along the strands and causes the ac copper loss to decrease, which ultimately, reduces the ac resistance.

V. Experimental Verification

In this section, the experiments to verify the analyzed results above are presented and conducted by using the fabricated E- and I- shaped core with winding specimens. The manufactured model and strands arrangements of winding specimens are shown in Fig. 17. First, the experimental set and procedure are explained in detail. Then, the tested results of resistance factor are obtained and investigated with FEA results.

A. Experimental Set and Procedure

Fig. 17(a) shows the manufactured model to be used for experiment to measure ac resistance. Each part, such as E- & I- shaped core, winding specimen, spacer, jig & bed, and thermocouple, of the manufactured model can be classified as three main roles for proper experiment, which are as follows.

1) E- and I- shaped core & Winding specimen: express the electric machines briefly.
2) Spacer & Jig & Bed: keep airgap length of 1 mm and prevent generating mechanical output.
3) Thermocouple: maintain the temperature when testing.

When applying the alternating current to manufactured model, the copper loss and iron loss are generated simultaneously. Therefore, the iron loss must be separated first to measure the ac resistance. It means that the 2-types of winding specimens are needed, and those are litz wire to separate the iron loss and round wire to measure ac resistance as shown in Fig. 17(b). All the winding specimens are manufactured to have the same number of turns as 15 and the same dc resistance for coil side. On the other hand, the reason why the litz wire is used to separate the iron loss is that the litz wire is composed of numerous strands with small diameter of strands and those are transposed, so that the ac resistance can be ignored.

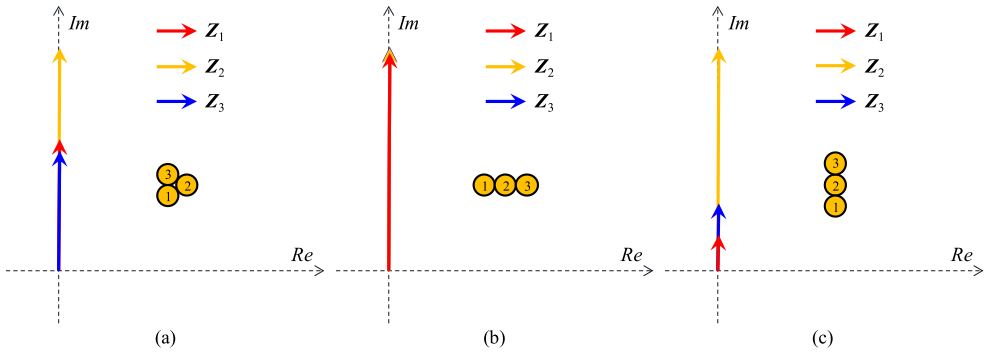

Fig. 12. Impedances of each strand at 2000 Hz (FEA). (a) 3 - *a*. (b) 3 - *b*. (c) 3 - *c*.

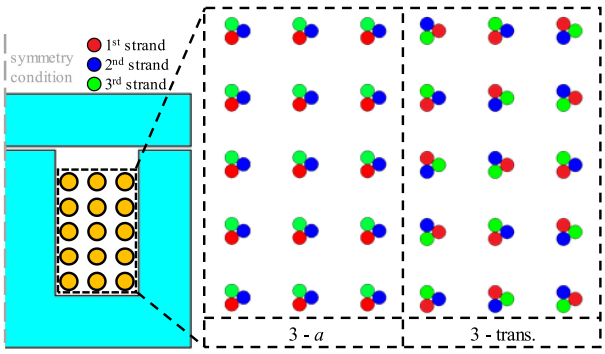

Fig. 13. Strand arrangement before and after applying transposition for three strands.

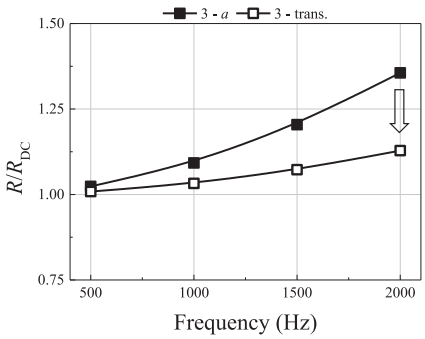

Fig. 14. FEA results of R/R_{DC} before and after applying transposition.

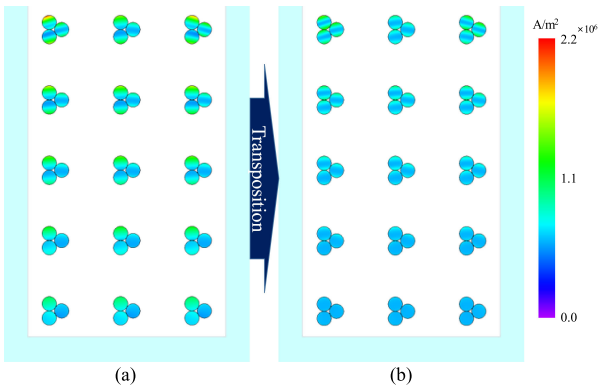

Fig. 15. RMS value of current density for conductors before and after applying transposition at 2000 Hz (FEA). (a) 3 - *a*. (b) 3 - trans.

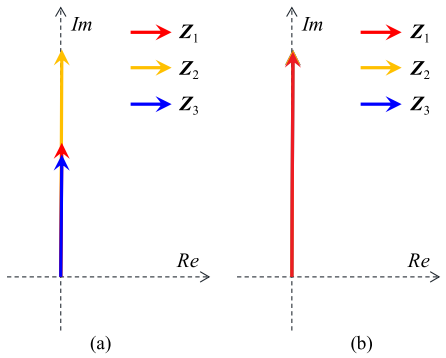

Fig. 16. Impedance of each strand at 2000 Hz (FEA). (a) 3 - *a*. (b) 3 - trans.

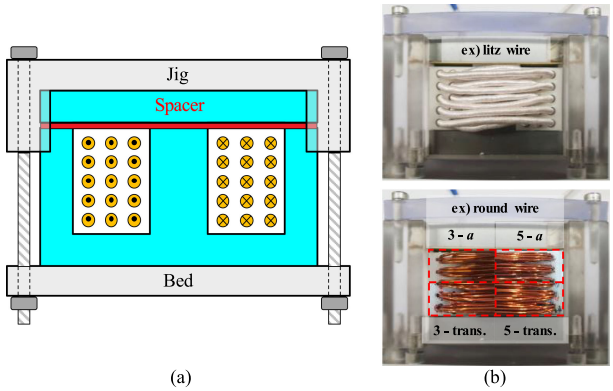

Fig. 17. E- and I- shaped core with winding specimens. (a) Simplified model. (b) Manufactured model with various winding specimens.

Fig. 18(a) shows the experimental set. The manufactured model, ac power supply, power analyzer, and multirecorder are used. The sinusoidal current of $24A_{rms}$ with frequency of 1100 Hz is applied by ac power supply and the input power, composed of copper loss and iron loss, is measured by power analyzer. Moreover, all the tests are conducted maintaining the constant temperature using thermocouple and multirecorder.

The procedure of experiment to measure the ac resistance is shown in Fig. 18(b). First, the winding specimen of litz wire is used to separate the iron loss under the same condition above and the input power, which represents the sum of copper loss and iron loss, is measured by the power analyzer. By multiplying

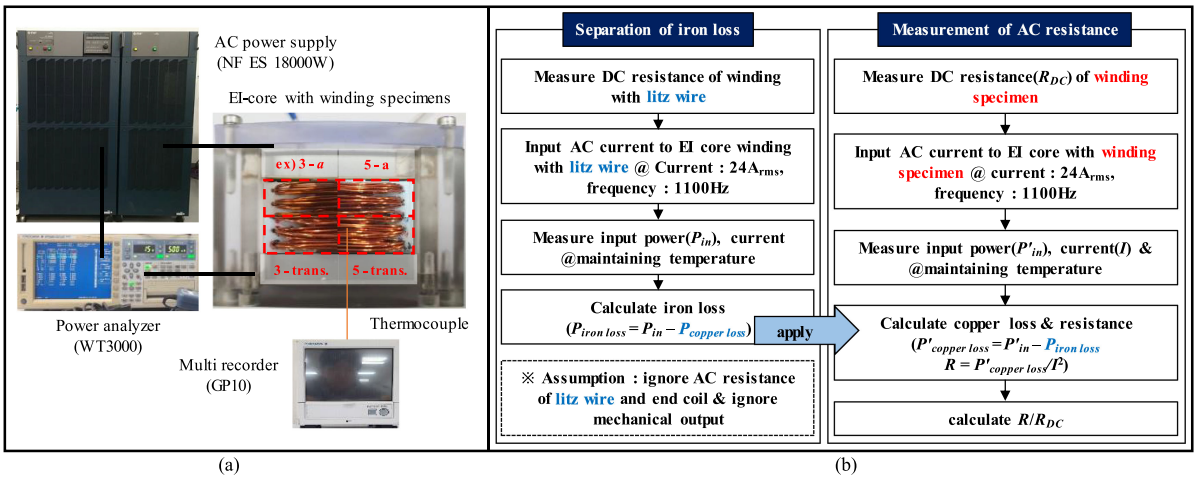

Fig. 18. Experimental set and procedure for measuring ac resistance of winding specimens wound with E- and I- shaped core. (a) Test set. (b) Test procedure.

the square of the rms current input and dc resistance of litz wire, the copper loss can be calculated since ac resistance of litz wire can be neglected as mentioned before. Then, the iron loss of the manufactured model can be separated by subtracting copper loss from input power. Next, the measurement of ac resistance according to the number and the arrangement of strands is performed. The winding specimens of round wire in Fig. 17(b) are used. Since the ac resistance of round wire cannot be ignored, there is additional loss by ac resistance. Therefore, the copper loss on winding specimen of round wire is calculated by subtracting the separated iron loss from the measured input power. Then, the ac resistance can be calculated by dividing the copper loss into the square of rms current input.

B. Separation of Iron Loss

The amplitude and the frequency of input current were $24A_{rms}$ and 1100 Hz, respectively. The measured total loss by power analyzer was 67.6 W and the copper loss was 9.6 W, calculated by multiplying the square of current and dc resistance of litz wire. Therefore, the separated iron loss was 58.0 W by subtracting the copper loss from the measured total loss. The separated iron loss will be used when measuring the ac resistance in the following section.

C. Measurement of AC Resistance According to the Configuration of Strands

To investigate the ac resistance according to the configuration of strands, the winding specimens of the number of strands 3 and 5 were manufactured. Both nontransposed and transposed winding specimens of those were manufactured to verify the effect of transposition as shown in Fig. 17(b).

Fig. 19 exhibits the results of testing ac resistance according to the configuration of strands. To apply the separated iron loss measured in the previous section, the same condition of current was supplied. With respect to the test results, the ac resistance of nontransposed cases according to the number of strands was almost the same. For the both cases, strands 3 and 5 showed the resistance factor of 1.25 approximately. However, when

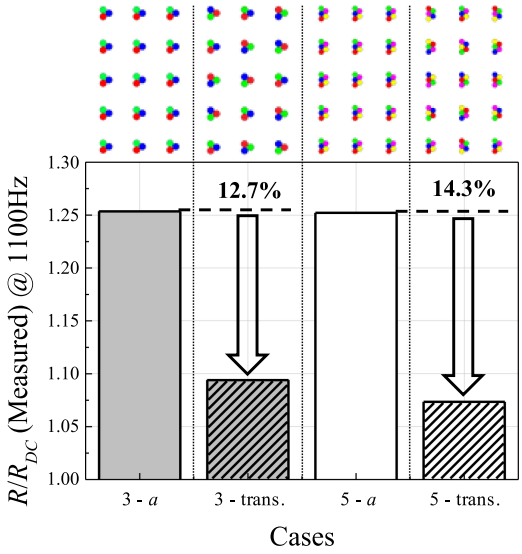

Fig. 19. R/R_{DC} results measured by test. @ 1100 Hz.

the transposition was applied, the resistance factor of strands 3 was 1.09, which was 12.7% decreased result compared to nontransposed, and that of strands 5 was 1.075, which was 14.3% decreased result with respect to non-ransposed.

Through the test results, the analyzed results of previous sections were verified and summarized as follows.

1) The number of strands has little effect on the ac resistance.
2) By transposing the arrangement of strands, the ac resistance decreased considerably with the removal of the circulating current generated by the unbalanced impedance of each strands.
3) Therefore, the arrangement of strands is remarkably more important than the number of strands for reducing ac resistance.

For example, this study can be a reference to the winding manufacturers that it is not recommended to arrange the strands in direction of crossing the slot leakage flux (the same direction along the tooth). Also, if winding manufacturers want to achieve

the effect of transposition, not only the perfect strand-by strand transposition but also the partial transposition, such as twisted, can reduce the ac resistance considerably.

Moreover, when operating the electric machines, the pulsewidth modulation (PWM) is widely used to excite sinusoidal current. Since the PWM generates harmonics in the current, the eddy current in winding that increases the ac resistance gets larger. Consequently, the arrangement of strands avoiding the increase of ac resistance is essential in electric machines.

VI. Conclusion

Considering the need for high speed and high voltage in the electric machine industry, this study investigated ac resistance on windings surrounded by an iron core for different strand configurations. To assume a similar condition as in electric machines, such as transformers, motors, and generators, the ac resistance of windings with E- and I- shaped core was investigated. The process of generating ac resistance was discussed from the slot leakage flux to the eddy current when the strands are not applied to the winding. Moreover, the change in ac resistance with the use of strands was discussed considering the inequivalence of impedance between each strand. To avoid this additional ac resistance, transposition, which makes the impedance of each strand equal, was proposed. Finally, the phenomena of ac resistance were analyzed by analytic method, FEA and were verified experimentally. The results show that the arrangement of strands is much more significant than the number of strands for reducing ac resistance. In addition, the transposition was effective in reducing the ac resistance. As mentioned above, situations analogous to electric machines were considered in this study. Therefore, it is important to arrange strands properly to avoid a critical rise in the ac resistance when the system of electric machines has a high frequency or high speed, not only for transformers but also for rotating machines, such as motor and generator.

References

[1] J. Chin, K. Cha, J. Park, J. Hong, and M. Lim, "Study on AC resistance of winding according to configuration of strands," in *Proc. IEEE Energy Convers. Congr. Expo.*, 2019, pp. 3137–3143.

[2] M. Lim, S. Chai, J. Yang, and J. Hong, "Design and verification of 150-krpm PMSM based on experiment results of prototype," *IEEE Trans. Ind. Electron.*, vol. 62, no. 12, pp. 7827–7836, Dec. 2015.

[3] J. Chin, S. Hwang, H. Park, and J. Hong, "Thermal analysis and verification of PMSM using LPTN considering mechanical components and losses," in *Proc. 13th Int. Conf. Elect. Mach.*, 2018, pp. 1323–1329.

[4] A. Boglietti, A. Cavagnino, and D. Staton "Determination of critical parameters in electrical machine thermal models," *IEEE Trans. Ind. Appl.*, vol. 44, no. 4 pp. 1150–1159 Jul./Aug. 2008.

[5] N. Simpson, R. Wrobel, and P. H. Mellor, "Estimation of equivalent thermal parameters of impregnated electrical windings," *IEEE Trans. Ind. Appl.*, vol. 49, no. 6, pp. 2505–2515, Nov./Dec. 2013.

[6] C. Paar, A. Muetze, and H. Kolbe, "Influence of machine integration on the thermal behavior of a PM drive for hybrid electric traction," *IEEE Trans. Ind. Appl.*, vol. 51, no. 5, pp. 3914–3922, Sep./Oct. 2015.

[7] I. Petrov, M. Polikarpova, P. Ponomarev, P. Lindh, and J. Pyrhönen, "Investigation of additional AC losses in tooth-coil winding PMSM with high electrical frequency," in *Proc. 22nd Int. Conf. Elect. Mach.*, 2016, pp. 1841–1846.

[8] M. Paradkar and J. Böcker, "Analysis of eddy current losses in the stator windings of IPM machines in electric and hybrid electric vehicle applications," in *Proc. 8th IET Int. Conf. Power Electron. Mach. Drives*, 2016, pp. 1–5.

[9] J. Chin, K. Cha, E. Lee, S. Park, J. Hong, and M. Lim, "Design of PMSM for EV traction using MSO coil considering AC resistance according to current density and parallel circuit," in *Proc. IEEE Veh. Power Propulsion Conf.* , 2019, pp. 1–6.

[10] K. Cha, J. Chin, E. Lee, S. Park, J. Hong, and M. Lim, "AC resistance reduction design of traction motor for high energy efficiency of electric vehicle," in *Proc. IEEE Veh. Power Propulsion Conf.*, 2019, pp. 1–6.

[11] N. Bianchi and G. Berardi, "Analytical approach to design hairpin windings in high performance electric vehicle motors," in *Proc. IEEE Energy Convers. Congr. Expo.*, 2018, pp. 4398–4405.

[12] G. Berardi and N. Bianchi, "Design guideline of an AC hairpin winding," in *Proc. 13th Int. Conf. Elect. Mach.*, 2018, pp. 2444–2450.

[13] F. Jiancheng, L. Xiquan, B. Han, and K. Wang, "Analysis of circulating current loss for high-speed permanent magnet motor," *IEEE Trans. Magn.*, vol. 51, no. 1, Jan. 2015, Art. no. 8200113.

[14] M. van der Geest, H. Polinder, J. A. Ferreira, and D. Zeilstra, "Current sharing analysis of parallel strands in low-voltage high-speed machines," *IEEE Trans. Ind. Electron.*, vol. 61, no. 6, pp. 3064–3070, Jun. 2014.

[15] D. C. Hanselman and W. H. Peake, "Eddy-current effects in slot-bound conductors," *IEE Proc. Elect. Power Appl.*, vol. 142, no. 2, pp. 131–136, Mar. 1995.

[16] T. A. Lipo, *Introduction to AC Machine Design*, 2nd ed. Madison, WI, USA: Wisconsin Power Electron. Res. Center, Univ. Wisconsin, 2004.

[17] J. Pyrhonen, T. Jokinen, and V. Hrabovcova, *Design of Rotating Electrical Machines*, 2nd ed. Hoboken, NJ, USA: Wiley, 2013.

[18] Y. Liang, Y. Wang, Y. Liu, and M. Fu, "Derivation of temperature distribution of stator winding with transposed conductors for a large air-cooled hydrogenerator," *IEEE Trans. Ind. Electron.*, vol. 63, no. 8, pp. 4764–4772, Aug. 2016.

[19] B. Xia, G. G. Jeong, and C. S. Koh, "Co-kriging assisted PSO algorithm and its application to optimal transposition design of power transformer windings for the reduction of circulating current loss," *IEEE Trans. Magn.*, vol. 52, no. 3, Mar. 2016, Art. no. 7208604.

[20] R. P. Wojda and M. K. Kazimierczuk, "Winding resistance and power loss of inductors with litz and solid-round wires," *IEEE Trans. Ind. Appl.*, vol. 54, no. 4, pp. 3548–3557, Jul./Aug. 2018.

[21] M. Vetuschi and F. Cupertino, "Minimization of proximity losses in electrical machines with tooth-wound coils," *IEEE Trans. Ind. Appl.*, vol. 51, no. 4, pp. 3068–3076, Jul./Aug. 2015.

Jun-Woo Chin received the bachelor's degree in mechanical engineering from Hanyang University, Seoul, South Korea, in 2014. He is currently working toward the Ph.D. degree in automotive engineering from Hanyang University.

His research interests include the design of electric machines for automotive, losses and thermal analysis of electric motor and generator.

Kyoung-Soo Cha received the bachelor's degree in electrical engineering from Chungbuk University, Cheongju, South Korea, in 2015. He is currently working toward the Ph.D. degree in automotive engineering from Hanyang University, Seoul, South Korea.

His research interests include electric machine design for automotive, home appliance, and rare-earth free machine.

Jin-Cheol Park received the bachelor's degree in electrical engineering from Chungbuk University, Cheongju, South Korea, in 2015. He is currently working toward the Ph.D. degree in automotive engineering from Hanyang University, Seoul, South Korea.

His research interests include electric machine design for automotive and numerical analysis of electromagnetic.

Dong-Min Kim received the B.S. degree in electronic information systems engineering from Hanyang University, Ansan, South Korea, in 2013. He is currently working toward the Ph.D. degree in automotive engineering from the Hanyang University, Seoul, South Korea.

His research interests include the design of electric machines for automotive and industrial applications, and modeling of electric vehicles and hybrid electric vehicles.

Jung-Pyo Hong (Senior Member, IEEE) received the Ph.D. degree in electrical engineering from Hanyang University, Seoul, South Korea, in 1995.

From 1996 to 2006, he was a Professor with Changwon National University, Changwon, South Korea. From 2006 to 2019, he had been a Professor with the Hanyang University, Seoul, South Korea.

His research interests included the design of electric machines, optimization and numerical analysis of electromechanics.

Myung-Seop Lim (Member, IEEE) received the bachelor's degree in mechanical engineering and the master's and Ph.D. degrees in automotive engineering from Hanyang University, Seoul, South Korea, in 2012, 2014, and 2017, respectively.

From 2017 to 2018, he was a Research Engineer with Hyundai Mobis, Yongin, South Korea. From 2018 to 2019, he was an Assistant Professor with Yeungnam University, Daegu, South Korea. Since 2019, he has been with Hanyang University, Seoul, South Korea, where he is currently an Assistant Professor.

His research interests include electromagnetic field analysis and multiphysics analysis of electric machinery for mechatronics systems such as automotive and robot applications.